Res Chem Intermed (2014) 40:1753–1770
DOI 10.1007/s11164-013-1078-3

Sorption of Bi^{3+} from acidic solutions using nano-hydroxyapatite extracted from Persian corals

S. Zamani · E. Salahi · I. Mobasherpour

Received: 17 November 2012 / Accepted: 23 January 2013 / Published online: 21 February 2013

Abstract Nano-crystallite hydroxyapatite (nano-HAp) synthesized from Persian corals was used for removing Bi^{3+} from acidic aqueous solutions. The effects of initial concentration, adsorbent dosage, contact time and temperature were studied in batch experiments. The sorption of Bi^{3+} by nano-HAp increased as the initial concentration of bismuth ion increased in the medium. The pseudo-first-order, pseudo-second-order and intraparticle diffusion kinetic models were applied to study the kinetics of the sorption processes. The pseudo-second-order kinetic model provided the best correlation ($R^2 > 0.999$) of the used experimental data compared to the pseudo-first-order and intraparticle diffusion kinetic models. Various thermodynamic parameters, such as ΔG°, ΔH° and ΔS° were calculated. Thermodynamics of Bi^{3+} cation sorption onto nano-HAp system pointed at spontaneous and endothermic nature of the process. The maximum Bi^{3+} adsorbed was found to be 3,333.33 mg g^{-1}. It was found that the sorption of Bi^{3+} on nano-HAp correlated well ($R^2 = 0.979$) with the Langmuir equation as compared to Freundlich and Dubinin–Kaganer–Radushkevich (D-K-R) isotherm equations under the concentration range studied. This study indicated that nano-HAp extracted from Persian corals could be used as an efficient adsorbent for removal of Bi^{3+} from acidic aqueous solution.

Keywords Sorption · Bi^{3+} · Nano-hydroxyapatite · Thermodynamic · Kinetic

S. Zamani · E. Salahi · I. Mobasherpour (✉)
Ceramics Department, Materials and Energy Research Center, P.O. Box 31787-316, Karaj, Iran
e-mail: i.mobasherpour@merc.ac.ir; iman.mobasherpour@gmail.com

Introduction

In the Earth's crust, bismuth presents at trace concentration (8 μg kg^{-1}) while bismuth minerals rarely occur alone and are almost always associated with other ores [1]. Bismuth is found in nature in the trivalent state as bismuthinite, Bi_2S_3, bismite, Bi_2O_3 and bismuth sulfide–telluric, Bi_2Te_2S. It is also found as a secondary component in some lead, copper and tin minerals [2]. Bismuth appears to be environmentally significant because its physical and chemical properties have led it to be used in different areas of life. Pamphlett et al. [3] has reported that bismuth compounds after oral intake enter the nervous system of mice, in particular, in motor neurons. Hence, bismuth species are included in the list of potential toxins [3]. As Bi^{3+} species are included in the list of potential toxins for motor neurons, a fast and selective method for removal of Bi^{3+} species has been developed [3].

Many methods have been developed to remove toxic metals from wastewater, namely adsorption, chemical oxidation/reduction, precipitation, ion exchange, electrochemical processes, membrane filtration and reverse osmosis. Among these methods, metal cation adsorption is quite promising due to its high efficiency, easy handling, availability of different adsorbents and cost effectiveness.

Calcium hydroxyapatite (Ca-HAp), $Ca_{10}(PO_4)_6(OH)_2$, has also been used for the removal of heavy and toxic metals from contaminated soils, wastewater and fly ashes [4–11]. Calcium hydroxyapatite is a principal component of hard tissues and has been of interest in industry and medical fields. Its synthetic particles find many applications in bioceramic, chromatographic adsorbents to separate proteins and enzymes, ascatalysts for dehydration and dehydrogenation of alcohols, methane oxidation, and powders for artificial teeth and bones paste germicides [12]. These properties relate to various surface characteristics of HAp, e.g., surface functional groups, acidity and basicity, surface charge, hydrophilicity, and porosity. It has been found that the Ca-HAp surface possesses 2.6 groups nm^{-2} of P–OH groups acting as sorption sites [13]. The sorption properties of HAp are of great importance for both environmental processes and industrial purposes.

Hydroxyapatite is an ideal material for long-term containment of contaminants because of its high sorption capacity for actinides and heavy metals, low water solubility, high stability under reducing and oxidizing conditions, availability, and low cost [4]. HAp has been utilized in the stabilization of a wide variety of metals (e.g., Cr, Co, Cu, Cd, Zn, Ni, Pu, Pb, As, Sb, U, and V) by many investigators [14–18]. They have reported that the sorption is taking place through ionic exchange reaction, surface complexation with phosphate, calcium and hydroxyl groups, and/or co-precipitation of new partially soluble phases.

The objective of this preliminary study was to investigate the feasibility of Bi^{3+} removal from acidic aqueous solution by HAp prepared by Persian corals. The dynamic behavior of adsorption was investigated regarding the effect of initial metal ion concentration, contact time, adsorbent mass and temperature of solution. The kinetics and thermodynamic parameters were also evaluated from the adsorption measurements. The Langmuir, Freundlich and D-K-R models were used to fit the equilibrium isotherm.

Materials and methods

Preparation of nano-crystallite hydroxyapatite sorbents

The coral was gathered from the southern coast of Kish Island in the Persian Gulf. The calcareous biomaterial that constitutes coral skeleton is made up of 99 % calcium carbonate and the rest is amino acids and oligo elements [19]. Natural coral was crushed and subsequently ground in an agate mortar. The powders were washed in distillated water. After drying, powders were heated to 900 °C for 1 h. The produced powders were then mixed with 2.5 times of diammonium hydrogen phosphate [$(NH_4)_2HPO_4$; Merck No. 1205)] by weight and distilled water. The resulting mixture converted to nano-HAp by the hydrothermal method. Hydrothermal conversion was carried out in a stainless steel reactor at 200 °C for 6 h. The precipitated product was washed with distillated water and dried at 80 °C for 24 h. The chemical reaction that took place is as follows [19]:

$$10CaCO_3 + 6(NH_4)_2HPO_4 + 2\ H_2O \rightarrow Ca_{10}(PO_4)_6(OH)_2 + 6(NH_4)_2CO_3 + 4\ H_2CO_3$$

The crystal phase was identified by powder X-ray diffraction (XRD) using a Siemens diffractometer (30 kV and 25 mA) with Cu Kα radiation. Fourier-transform infra-red (FTIR) analysis was conducted using a Bruker Vector 33 FT-IR spectrometer. KBr was used for preparing of pellet-shaped samples and tests were performed according to ASTM 1252. The specific surface area producing nano-HAp was determined by the BET-method (Micromeritics Gemini 2375, adsorption gas N_2, carrier gas He). SEM micrographs were prepared by using Cam Scan MV2300 SEM (with 15 kV accelerating voltage).

Sorption study

All sorption experiments were carried without imposing any pre-equilibration processes during the performance of any experiments. Using a batch equilibration technique, the sorption capacity of nano-HAp extracted from corals for Bi^{3+} cation, as well as the influence of the initial concentration of Bi^{3+} cation, adsorbent mass, contact time and temperature, sorption experiments, was determined. For the evaluation of equilibrium performance, a volume of acid solution containing the appropriate concentration of Bi^{3+} was mixed with a known amount of nano-HAp. The slurry was agitated for 120 min to be certain of reaching equilibrium. The initial pH of solution was adjusted to the value of 1.5 by using HCl 0.01 M in all experiments. The desired pH of the solutions was maintained by adding HCl at the beginning of the experiment and not controlled afterwards.

Acidic aqueous solutions containing Bi^{3+} cation of concentrations 50, 150, 175, and 200 mg L^{-1} were prepared from bismuth oxide (Bi_2O_3; Merck No.2026). Then, 0.02 g of nano-HAp extracted from corals was introduced into a stirred tank reactor containing 500 mL of the prepared solution. The agitator stirring speed was 700 rpm. The temperature of the suspension was maintained constant at 25 ± 1 °C. Samples were taken after mixing the adsorbent and Bi^{3+} cation-bearing solution at

pre-determined time intervals (5, 10, 20, 30, 60, and 120 min) for the measurement of residual metal ion concentration in the solution and to ensure equilibrium was reached. The sample volume taken was 2 mL. After each specified time, the sorbents were separated from the solution by centrifuge and filtration through filter paper (Whatman grade 6). The exact concentration of metal ions was determined by AAS (GBC 932 Plus atomic absorption spectrophotometer). Two replicates were used for each Bi^{3+} sorption experiment and the results given were the average values. The mass balance of bismuth is given by:

$$mq = V(C_0 - C) \tag{1}$$

where m, q, V, C_0, and C are the mass of nano-HAp (g), amount of bismuth removed by unit of weight of HAp (uptake capacity: mg Bi/g HAp), volume of bismuth solution (L), initial bismuth concentration of solution (mg Bi/L), and the concentration of bismuth at the time t of adsorption (mg Bi/L), respectively. After 120 min, C and q will reach equilibrium value C_e and q_e.

The percent removal (%) and distribution ratio (K_d) were calculated using the following equations.

$$\%\text{Removal} = \frac{(C_0 - C_f)}{C_0} \times 100 \tag{2}$$

where C_0 and C_f are the concentrations of the metal ion in initial and final solutions (after 120 min), respectively, and

$$K_d = \frac{\text{amount of metal in adsorbent}}{\text{amount of metal in solution}} \times \frac{V}{m} \tag{3}$$

where V is the volume of the solution (mL) and m is the weight of the adsorbent (g).

Results and discussion

Characteristics of adsorbent

The X-ray diffractograms of coral and synthesized HAp are shown in Fig. 1a, b, respectively. Corals that were used in this work (Fig. 1a) exhibit the presence of both aragonite and calcite phases that are two stable phases of the calcium carbonate in atmospheric and high pressures, respectively [20]. The XRD pattern in Fig. 1b shows that the reflection patterns matched the ICDD standards (JCPDS) for the HAp phase. The patterns only showed the peaks characteristic of HAp with no obvious evidence for the presence of other additional phases. In addition, no peaks corresponding to $CaCO_3$ or CaO connected to the initial coral were found. The broad peaks around the 211 and 002 planes indicated that the crystallites were very tiny in nature with much atomic oscillation. A SEM micrograph of the HAp extracted from coral powders is shown in Fig. 2. As can be seen from the morphologies of particles, there is a distribution of small particles and large agglomerates. These agglomerates consist of very fine particles (around 100 nm) that are cold-welded together. In order to explore the surface characteristics of the HAp particles, FT-IR analysis was performed and the

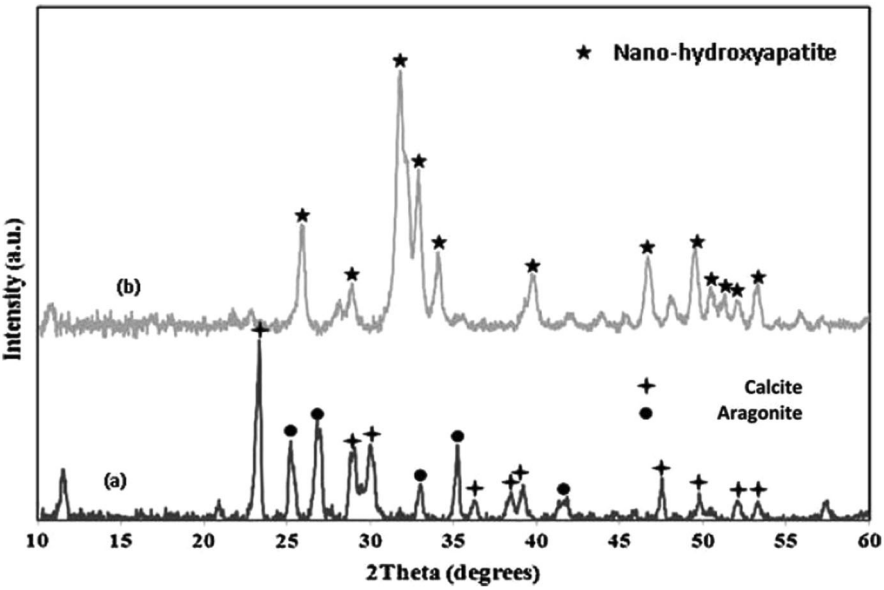

Fig. 1 XRD patterns of **a** Persian coral and **b** synthetic nano-calcium hydroxyapatite extracted from corals

revealed spectrum is given in Fig. 3. The FTIR of HAp extracted from corals shows adsorption bands at 562, 597, 962, 1,032, and 1,095 cm^{-1} corresponding to the PO_4^{3-} groups of the hydroxyapatite. The band around 3,650, 3,572 cm^{-1} and peaks around 632 cm^{-1} are due to the OH^- groups. However, the appearance of peaks at 1,460, 1,418 and 870 cm^{-1} indicate the presence of trace contamination of residual carbonate in HAp. As there was no $CaCO_3$ peak detected in the XRD pattern of nano-HAp, it is believed that this might have originated due to the ambient air atmosphere. The analysis of the HAp extracted from coral samplef has confirmed a nano-product, with the specific surface area 15.55 $m^2\ g^{-1}$.

Effect of initial Bi^{3+} concentration and adsorbent dosage

The sorption of Bi^{3+} cation was carried out at different initial bismuth concentrations ranging from 50 to 200 mg L^{-1}, at pH 1.5, at 700 rpm with 120 min of contact time using nano-HAp extracted from corals. A rapid kinetic reaction of Bi^{3+} removal by sorbent occurred within the first 5 min (Fig. 4a). The aqueous Bi^{3+} concentration at 5 min decreased to 23.25, 113, 127, and 151 mg L^{-1} by nano-HAp extracted from corals for 50, 150, 175, and 200 mg L^{-1} initial concentration, respectively. The uptake of the Bi^{3+} ion is increased by increasing the initial metal concentration tending to saturation at higher metal concentrations. As shown in Fig. 4b, when the initial Bi^{3+} cation concentration increased from 50 to 200 mg L^{-1}, the uptake capacity of nano-HAp increased from 1,675 to 3,050 mg g^{-1}. A higher initial concentration provided an important driving force to overcome all mass transfer resistances of the pollutant between the aqueous and solid phases thus increased the uptake [21].

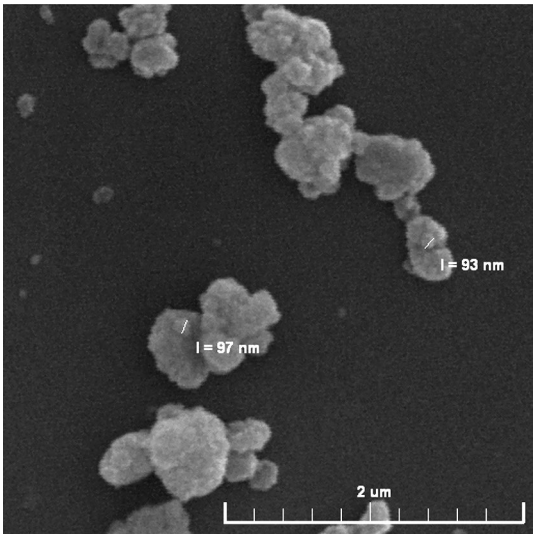

Fig. 2 SEM micrograph of nano-hydroxyapatite particles was prepared from Persian Gulf coral

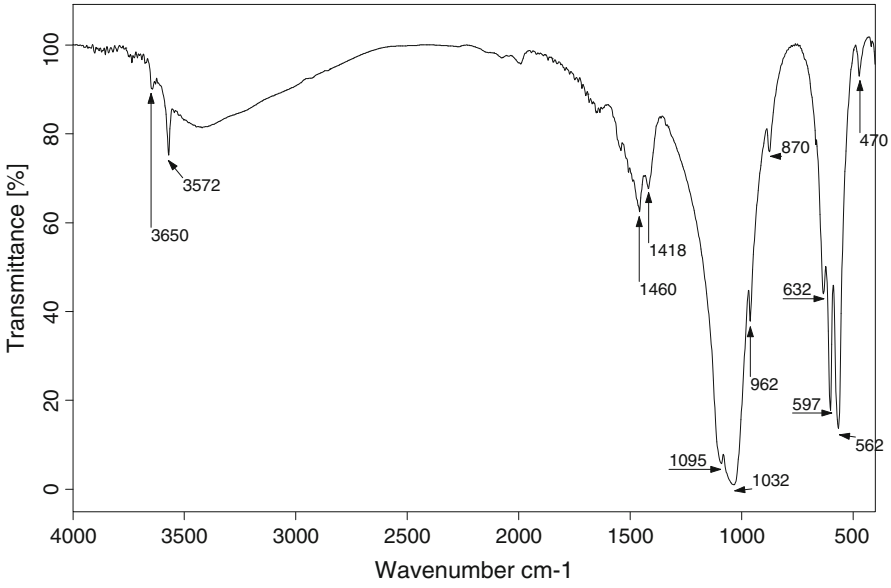

Fig. 3 FTIR spectra of synthetic nano-calcium hydroxyapatite extracted from corals

The effect of nano-HAp extracted from coral dosage is depicted in Fig. 5. Evidently, percentage removal increased with the increase of the sorbent mass (Fig. 5a) and the uptake capacity of Bi^{3+} decreased from 5,400 mg g^{-1} (27 % removal) to 2,750 mg g^{-1} (55 % removal) with increasing nano-HAp concentration from 0.01 to 0.04 g L^{-1} (Fig. 5b). This was attributed to a higher dosage of sorbent due to the increased surface area providing more adsorption sites available which gave rise to a higher removal of Bi^{3+} cation.

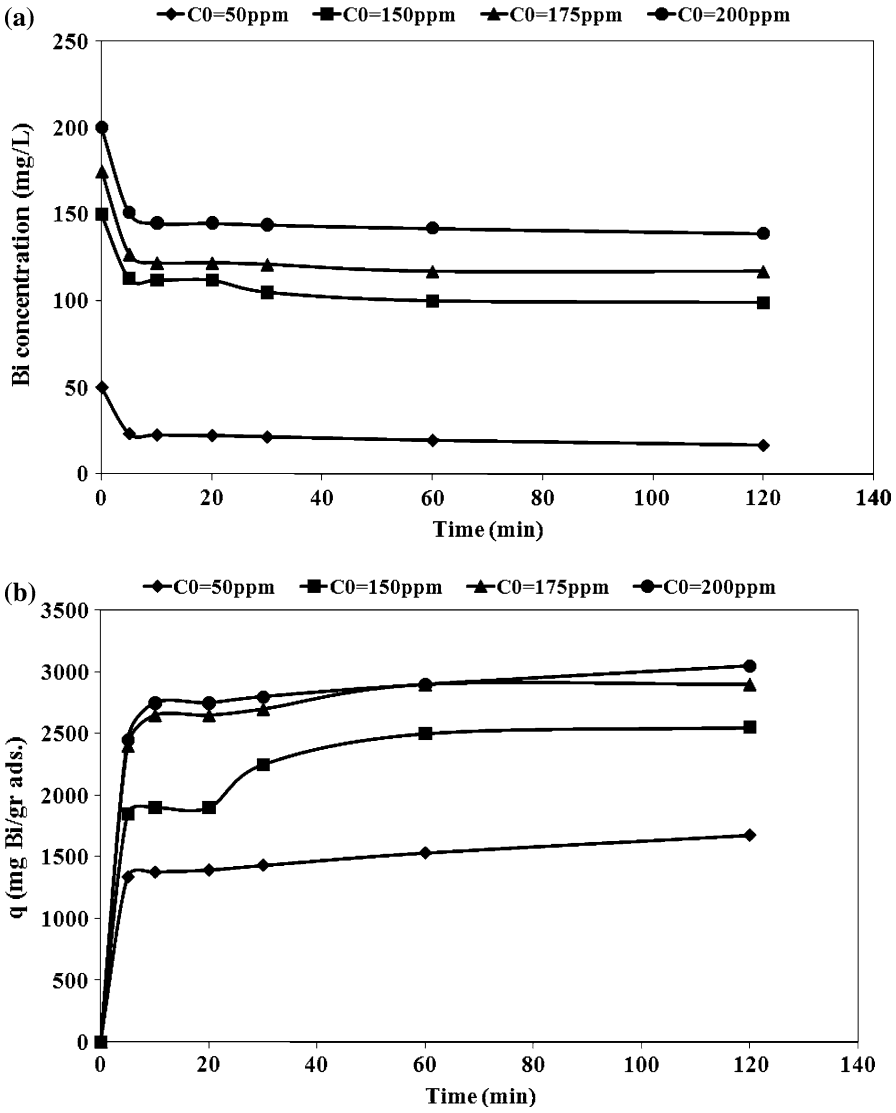

Fig. 4 Time dependent concentration of aqueous Bi^{3+} by nano-HAp sorbents (**a**), effect of initial concentration on removal of Bi^{3+} by nano-HAp sorbents (**b**) (pH 1.5, adsorbent dosage = 0.02 g L^{-1}, 700 rpm agitating rate)

Effect of contact time and sorption kinetic

The effect of contact time was studied using a solution containing 200 mg L^{-1} concentration of Bi^{3+} ion using nano-HAp extracted from corals at pH = 1.5 up to a contact time of 120 min. It seemed that the adsorption consisted of two phases: a primary rapid phase and a second slow phase. The first rapid phase lasted approximately 5 min and accounted for the major part in the total Bi^{3+} adsorption.

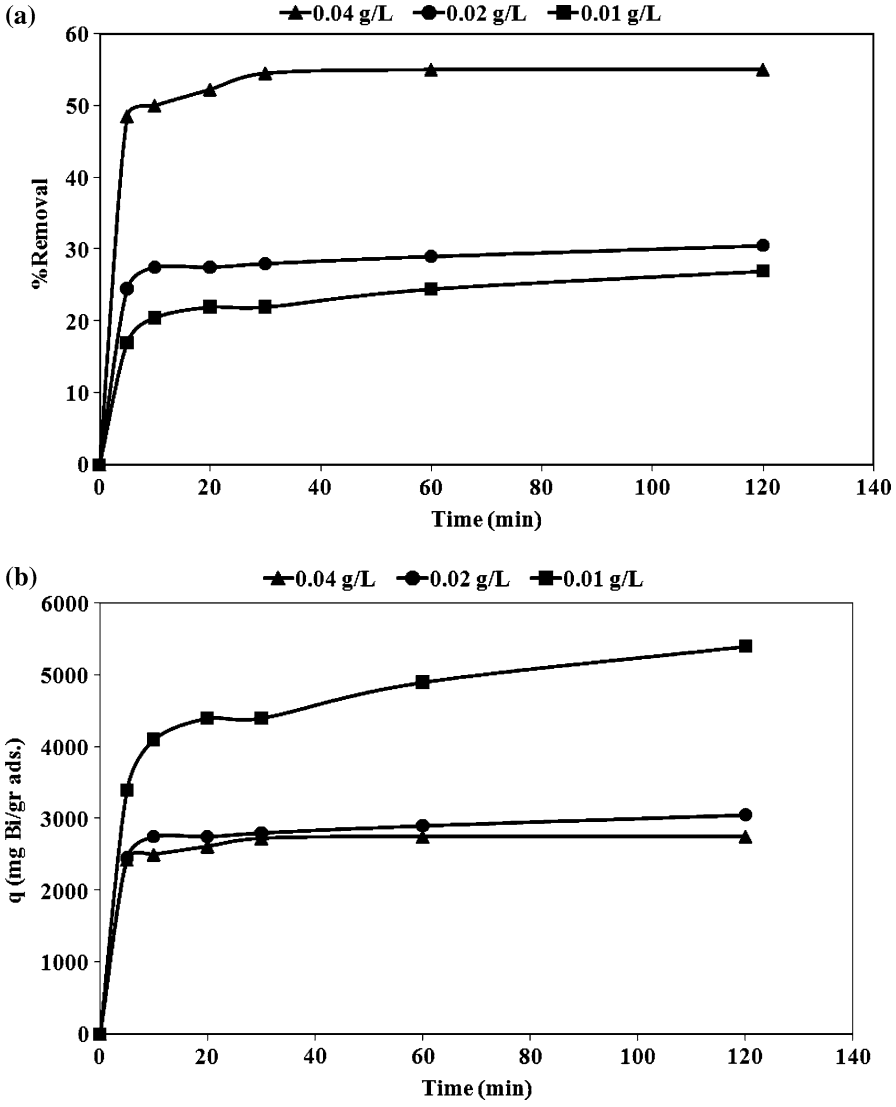

Fig. 5 Effect of adsorbent dosage on percentage removal (**a**) and uptake capacity (**b**) of Bi^{3+} by nano-HAp extracted from corals (pH 1.5, initial metal concentration = 200 mg L^{-1}, 700 rpm agitating rate)

Adsorption reached a plateau value in approximately 30 min, which showed saturation of the active points (Fig. 4b).

The sorption kinetics may be controlled by various diffusion mechanisms: (1) bulk diffusion, (2) film diffusion, and (3) intraparticle diffusion. Three models were used for the description of kinetic profiles based on the pseudo-first-order equation (the so-called Lagergren equation), on the pseudo-second-order equation described by Ho [27], and on the intraparticle diffusion model.

The pseudo-first-order equation of Lagergren can be expressed as Eq. (4):

$$log(q_e - q) = log\, q_{ecal} - \frac{k_1}{2.303} t \tag{4}$$

where q is the amount of metal ions adsorbed (mg g^{-1}) at any given time t (min), q_e is the amount of metal ion adsorbed (mg g^{-1}) at equilibrium and K_1 is the pseudo-first-order reaction rate constant for adsorption (min^{-1}). The pseudo-second-order reaction rate equation has the form:

$$\frac{t}{q_t} = \frac{1}{k_2 q_{e\ cal}^2} + \frac{t}{q_{e\ cal}} \tag{5}$$

where q_t is the amount of metal ions adsorbed (mg g^{-1}) at any given time t (min), q_e is the amount of metal ion adsorbed (mg g^{-1}) at equilibrium and K_2 is the second-order reaction rate constant for adsorption [g(mg min^{-1})].

The intraparticle diffusion model [22] was considered in order to determine the participation of this process in the sorption of bismuth ion by nano-HAp. According to this model, the plot of uptake (q_t), versus the square root of time ($t^{0.5}$) should be linear if intraparticle diffusion is involved in the overall adsorption mechanism. Furthermore, if this line passes through the origin then the intraparticle diffusion is the rate-controlling step of the process [23]. The initial rate of intraparticle diffusion, K_D, can be calculated in the following way:

$$q_t = K_D \times t^{0.5} \tag{6}$$

where q_t is the amount of sorbate on the surface of the sorbent at time t (mg g^{-1}), K_D is the intraparticle rate constant [mg(g $min^{0.5})^{-1}$] and t is the time (min).

Figure 6a, b shows linear plots of the pseudo-first-order model in Eq. (4) and the pseudo-second-order model in Eq. (5) for the adsorption of Bi^{3+} onto nano-HAp. K_1, K_2 and q_e calculated from the slopes and intercepts of the lines obtained by plotting log ($q_e - q_t$) against t and t/q_t against t are listed in Table 1. As shown in Table 1, the pseudo-second-order model fits the adsorption kinetics of bismuth ion on nano-HAp better than the pseudo-first-order model. This suggests that the rate-limiting step of this sorption system may be chemical sorption or chemisorptions involving valency forces through sharing or exchange of electrons between sorbent and sorbate [24, 25]. The q_e calculated from the pseudo-second-order rate model of Bi^{3+} is 3,086.42 mg g^{-1}. Figure 6c shows a plot of the Weber and Morris intraparticle diffusion model for the sorption of Bi^{3+} onto nano-HAp. As shown in Fig. 6c, the plot of uptake (q_t), versus the square root of time ($t^{0.5}$) was not linear, which indicated that the intraparticle diffusion was not the rate-controlling step in these adsorption systems.

Effect of temperature and determination of thermodynamic parameters

To study the effect of the temperature parameter on the uptake of Bi^{3+} cation by nano-HAp extracted from corals in acidic solution, temperatures of 25, 40, and

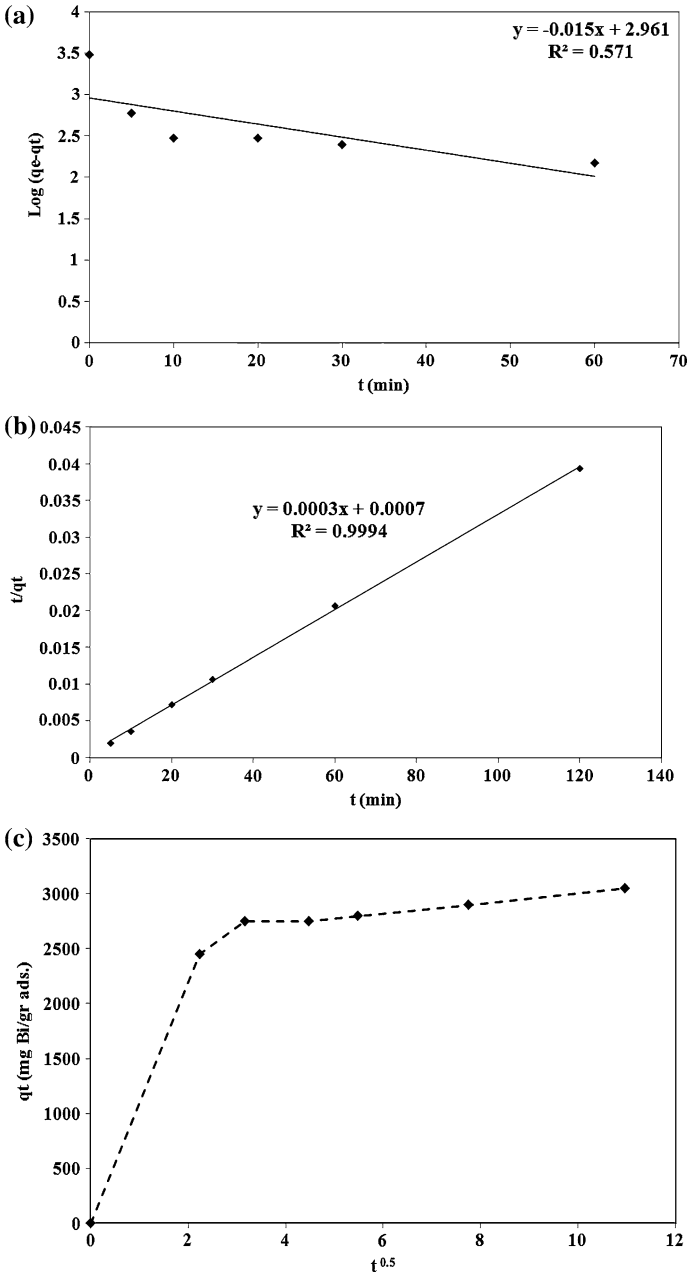

Fig. 6 Linear fit of experimental data obtained using **a** pseudo-first-order model and **b** pseudo-second-order model, and **c** the amount of single metal ion sorbed versus square root of time

60 °C were selected. Figure 7a illustrates the relationship between temperature and the amount of Bi^{3+} cation adsorbed onto nano-HAp at equilibrium time (120 min). As can be seen, the adsorption of Bi^{3+} cation on nano-HAp increased from

Table 1 Parameter values calculated using the pseudo-first-order and the pseudo-second-order models for the adsorption of Bi (HI) on nano-HAp extracted corals in acidic solutions

Temperature (°C)	K_1 (min^{-1})	$q_{e\ cal}$ (mg g^{-1})	R^2
Pseudo-first-order kinetic model			
25	0.03684	935.40	0.571
Pseudo-second-order kinetic model			
25	0.00014	3,086.42	0.999

3,050 mg g^{-1} (30.5 % removal) to 3,250 mg g^{-1} (32.5 % removal) when the temperature was increased from 25 to 60 °C at an initial concentration of 200 mg L^{-1}. The increase in the equilibrium sorption of Bi^{3+} cation with temperature indicated that Bi^{3+} cation removal by adsorption on nano-HAp favored a high temperature condition. This could be the result of an increase in the mobility of the Bi^{3+} cation with temperature. An increasing number of molecules could also acquire sufficient energy to undergo an interaction with active sites at the surface. Furthermore, increasing temperature may produce a swelling effect within the internal structure of the nano-HAp extracted from corals enabling large metal ions to penetrate further [26].

Thermodynamic parameters such as free energy (ΔG), enthalpy (ΔH), and entropy (ΔS) changes can be estimated using equilibrium constants changing as a function of temperature. The free energy changes of the sorption reaction are given by the following equation.

$$\Delta G = -RT \text{ Ln } K_d \tag{7}$$

where ΔG is free energy changes (J); R is the universal gas constant, 8.314 J mol^{-1} K^{-1} and T is the absolute temperature (K).

$$\Delta G = \Delta H - T\Delta S \tag{8}$$

The distribution ratio (K_d) values increased with raising temperature (Fig. 7b), indicating the endothermic nature of adsorption. A plot of Gibbs free energy changes,ΔG, versus temperature, T(K), was found to be linear. The values of ΔH and ΔS were determined from the slope and intercept of the plots. The thermodynamic parameters Gibbs free energy change, ΔG, are shown in Table 2. The enthalpy, ΔH, and the entropy changes,ΔS, for the sorption processes were calculated to be 2,243.34 J mol^{-1} and 84.81 J mol^{-1} K^{-1}, respectively. The negative values of ΔG at various temperatures indicated the spontaneous nature of the adsorption process. The positive value of ΔS indicated that there is an increment in the randomness in the system solid/solution interface during the adsorption process. In addition, the positive value of ΔH indicated that the adsorption was endothermic. The positive value of ΔS reflected the affinity of the nano-HAp for Bi^{3+} cation and suggested some structural changes in bismuth and nano-HAp extracted from corals [27].

Adsorption isotherms

Analysis of the equilibrium data is important to develop an equation which accurately represents the results and can be used for the design purposes [28]. Several isotherm equations have been used for the equilibrium modeling of adsorption systems.

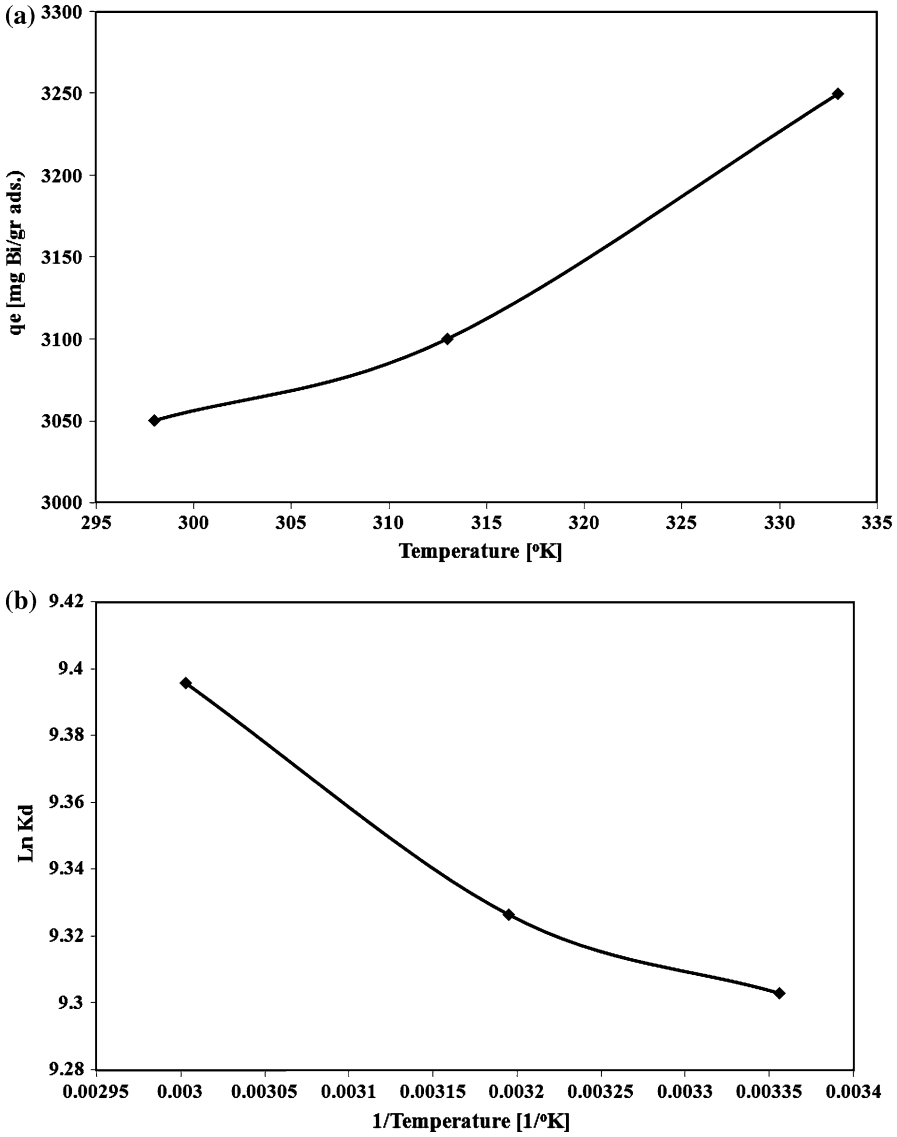

Fig. 7 The uptake capacity of Bi^{3+} ions at different temperature (**a**) and plot of ln K_d versus 1/T (**b**) (pH 1.5, initial metal concentration = 200 mg L^{-1}, adsorbent dosage = 0.02 g L^{-1}, 700 rpm agitating rate)

The sorption data have been subjected to different sorption isotherms, namely Langmuir, Freundlich, and Dubinin–Kaganer–Radushkevich (DKR).

The equilibrium data for metal ions over the concentration range from 50 to 200 mg L^{-1} at 25 °C were correlated with the Langmuir isotherm [29]:

Table 2 Thermodynamic parameters for the adsorption of Bi onto nano-HAp extracted corals in acidic solution

T (K)	K_d	ΔG (J mol^{-1})	ΔH (J mol^{-1})	ΔS (J mol^{-1} K^{-1})
298	10,971.22	−23,048.9		
313	11,231.88	−24,270.2	2,243.34	84.81
333	12,037.04	−26,012.7		

$$\frac{C_e}{q_e} = \frac{1}{Q_0 K} + \frac{C_e}{Q_0} \tag{9}$$

where C_e is the equilibrium concentration of metal in solution (mg L^{-1}), q_e is the amount absorbed at equilibrium onto nano-HAp extracted from corals (mg g^{-1}), Q_0 (mg g^{-1}), and K (L mg^{-1}) are Langmuir constants related to sorption capacity and sorption energy, respectively. Maximum sorption capacity (Q_0) represents monolayer coverage of sorbent with sorbate and K represents enthalpy of sorption and should vary with temperature. A linear plot was obtained when C_e/q_e was plotted against C_e over the entire concentration range of metal ions investigated.

The plotted Langmuir adsorption isotherms of Bi^{3+} cation are given in Fig. 8a. An adsorption isotherm is characterized by certain constants which values express the surface properties and affinity of the sorbent and can also be used to find the sorption capacity of sorbent.

The Freundlich sorption isotherm, one of the most widely used mathematical descriptions, usually fits the experimental data over a wide range of concentrations. This isotherm gave an expression encompassing the surface heterogeneity and the exponential distribution of active sites and their energies. The Freundlich adsorption isotherms were also applied to the removal of Bi^{3+} cation on nano-HAp in acidic solution (Fig. 4b).

$$\mathrm{Ln}q_e = \mathrm{Ln}k_f + \frac{1}{n}\mathrm{Ln}c_e \tag{10}$$

where q_e is the amount of metal ion adsorbed at equilibrium per gram of adsorbent (mg g^{-1}), C_e is the equilibrium concentration of metal ion in the solution (mg L^{-1}), and k_f and n are the Freundlich model constants [30, 31]. Freundlich parameters, k_f and n, were determined by plotting $\ln q_e$ versus $\ln C_e$. The numerical value of $1/n < 1$ indicates that adsorption capacity is only slightly suppressed at lower equilibrium concentrations. This isotherm does not predict any saturation of the sorbent by the sorbate; thus, infinite surface coverage is predicted mathematically, indicating multilayer adsorption on the surface [32].

The DKR equation has been used to describe the sorption of metal ions on clays. It has the form:

$$\mathrm{Ln}\ C_{ads} = \mathrm{Ln}\ X_m - \beta\varepsilon^2 \tag{11}$$

where C_{ads} is the number of metal ions adsorbed per unit weight of adsorbent (mol g^{-1}), X_m (mol g^{-1}) is the maximum sorption capacity, β (mol^2 J^{-2}) is the

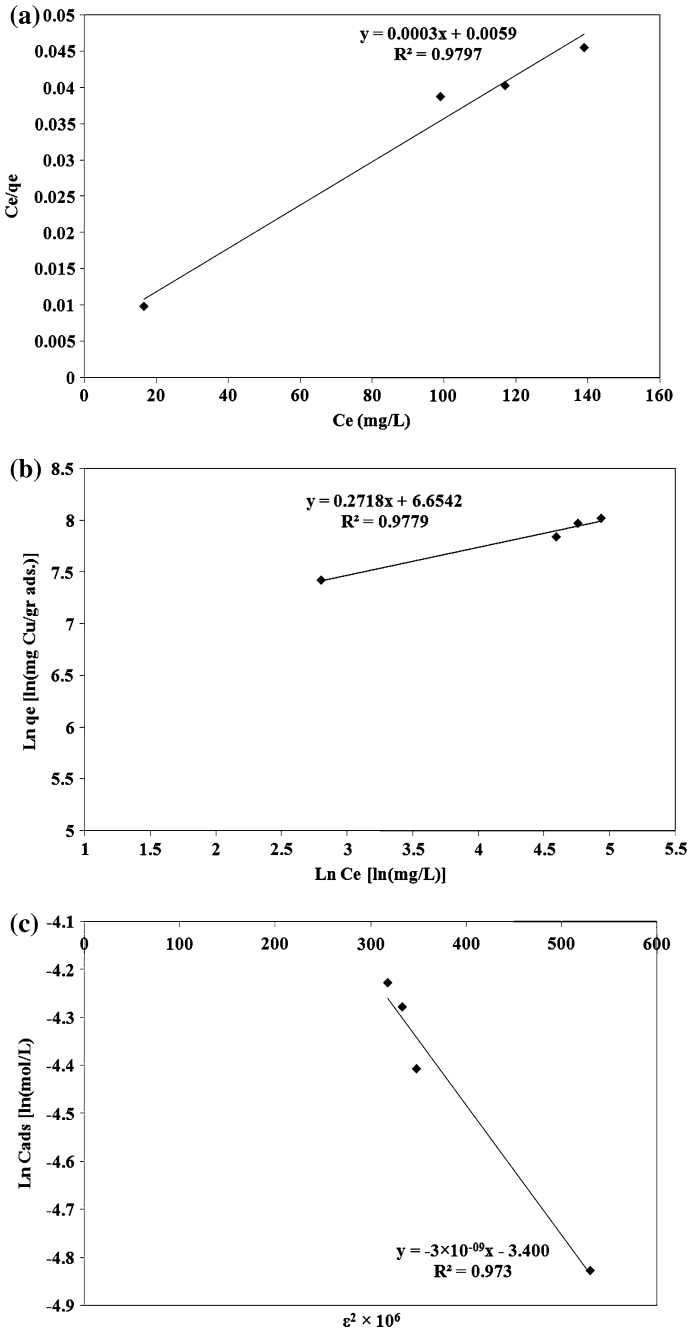

Fig. 8 Linear fits of experimental data obtained using Langmuir (**a**), Freundlich (**b**) and Dubinin–Kaganer–Radushkevich (**c**) sorption isotherms for the adsorption of Bi^{3+} onto nano-HAp extracted corals in acidic solution

activity coefficient related to mean sorption energy, and ε is the Polanyi potential, which is equal to:

$$\varepsilon = RT\ln(1 + 1/C_e) \tag{12}$$

where R is the gas constant (8.314 kJ mol^{-1} K^{-1}) and T is the temperature (K). The saturation limit X_m may represent the total specific micro-pore volume of the sorbent. The sorption potential is independent of the temperature but varies according to the nature of sorbent and sorbate [33]. The slope of the plot of ln C_{ads} versus ε^2 gives β (mol^2 J^{-2}) and the intercept yields the sorption capacity, X_m (mol g^{-1}). The sorption space in the vicinity of a solid surface is characterized by a series of equipotential surfaces having the same sorption potential. The sorption energy can also be worked out using the following relationship:

$$E = 1/\sqrt{-2\beta} \tag{13}$$

It is known that magnitude of apparent adsorption energy E is useful for estimating the type of adsorption and if this value is below 8 kJ mol^{-1} the adsorption type can be explained by physical adsorption, between 8 and 16 kJ mol^{-1} the adsorption type can be explained by ion exchange, and over 16 kJ mol^{-1} the adsorption type can be explained by a stronger chemical adsorption than ion exchange [34–36].

The plot of Ln C_{ads} against ε^2 for metal ion sorption on nano-HAp extracted from corals is shown in Fig. 8c. The Langmuir, Freundlich and DKR adsorption constants from the isotherms and their correlation coefficients are also presented in Table 3.

The correlation coefficients R^2 (0.979, 0.977 and 0.973 for Langmuir, Freundlich and DKR models, respectively) confirmed good agreement between both theoretical models and experimental results in the present study. The maximum sorption capacity, Q_0, calculated from the Langmuir equation was 3,333.33 mg g^{-1}, while the Langmuir constant, K, was 0.05 L mg^{-1}. The values obtained for Bi^{3+} cation from the Freundlich model showed a maximum adsorption capacity (K_f) of 776.03 mg g^{-1} with an affinity value (n) equal to 3.67. The values of sorption

Table 3 Langmuir, Freundlish and Dubinin–Kaganer–Radushkevich (*DKR*) constants for sorption of Bi onto nano-HAp extracted corals in acidic solution

Langmuir adsorption isotherms constants		
Q_0 (mg g^{-1})	K (L mg^{-1})	R^2
3,333.33	0.05	0.979
Freundlich adsorption isotherms constants		
k_f (mg g^{-1})	n	R^2
776.03	3.67	0.977
DKR adsorption isotherms constants		
X_m (mg g^{-1})	β (mol^2 J^{-2})	R^2
6,974.34	-3×10^{-9}	0.973

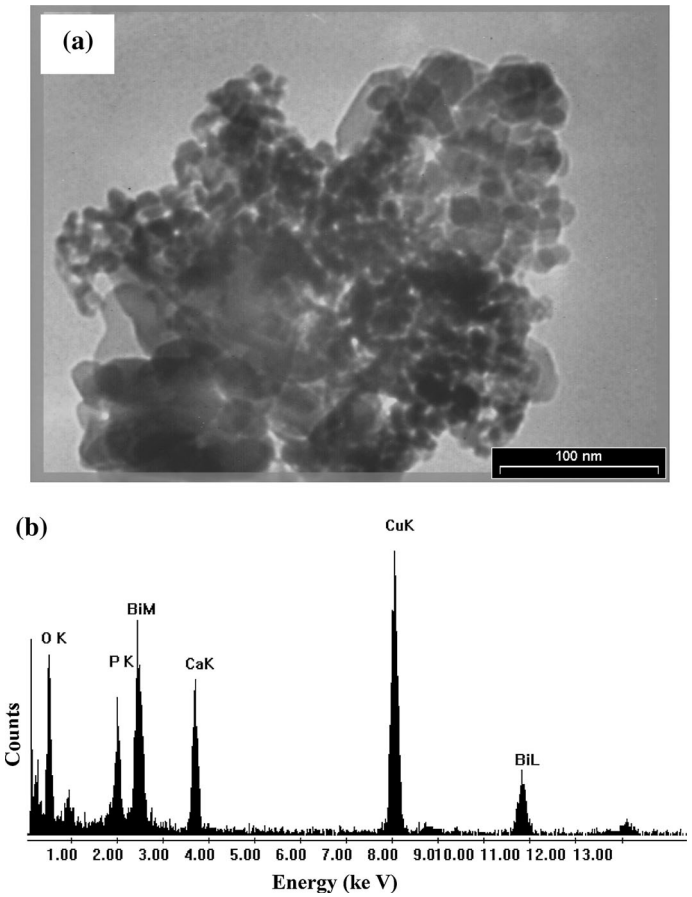

Fig. 9 TEM micrograph (**a**) and EDS spectrum (**b**) of the solid residue with maximum amount of uptake capacity of Bi^{3+}, respectively

constants, derived from DKR model, were 6,974.34 mg g^{-1} (33.37 mmol g^{-1}) for X_m, -3×10^{-9} mol^2 J^{-2} for β and 12.90 kJ mol^{-1} for E.

The values indicated that the adsorption pattern for Bi^{3+} cation on nano-HAp extracted from corals followed the DKR isotherm ($R^2 > 0.973$), the Freundlich isotherm ($R^2 > 0.977$) and the Langmuir isotherm ($R^2 > 0.979$) in all experiments. It is clear that the Langmuir isotherm best fitted the sorption of Bi^{3+} cations on nano-HAp extracted from corals in acidic solution. When the system is in a state of equilibrium, the distribution of Bi^{3+} cation between the nano-HAp and the Bi^{3+} solution is of fundamental importance in determining the maximum sorption capacity of nano-HAp for the bismuth ion from the isotherm. The E values are 12.90 kJ for Bi^{3+} cation on the nano-HAp extracted from corals. It is the orders of an ion-exchange mechanism, in which the sorption energy lies within 8–16 kJ mol^{-1}.

The TEM of Bi^{3+}-loaded sample particles is shown in Fig. 9a) indicating that most crystallines are rounded with dimensions in the range of 20–40 nm. No

morphology of nano-HAp-loaded Bi^{3+} was detected by the TEM crystalline analysis of the solid residue with maximum amount of uptake capacity of Bi^{3+}. Figure 9b shows the EDS spectrum and powder diffraction pattern of the Bi^{3+}-loaded sample particles. Clear peaks corresponding to Ca, P, O and Bi were observed in the EDS spectrum. The EDS spectrum confirms its chemical composition and the powder diffraction pattern further validate the crystallinity of the synthesized powder. In addition, Cu peaks were also observed in the EDS spectrum. The peaks for Cu arise from stray scattering of X-rays from the copper grid.

Conclusions

The present investigation showed that the nano-HAp extracted from corals was an effective adsorbent for the removal of Bi^{3+} cation from acidic aqueous solutions. The adsorption process was a function of the adsorbent dosage, initial Bi^{3+} cation concentration, contact time, and temperature. The efficiency of Bi^{3+} cation adsorption increased with an increase in the adsorbent dosage. Thermodynamic calculations showed that the bismuth sorption process of nano-HAp extracted from corals had endothermic and spontaneous nature. The pseudo-first-order, pseudo-second-order kinetic and intraparticle diffusion kinetic models were used to describe the kinetic data for initial Bi^{3+} concentrations and the rate constants were evaluated. The used experimental data were fitted by the second-order kinetic model, which indicated that chemical sorption was the rate-limiting step, inside of mass transfer. The contact time of approximately 30 min was required to reach the equilibrium. Isotherm studies indicated that the Langmuir model fitted the experimental data better than Freundlich and DKR models. The adsorption equilibrium was described well by the Langmuir isotherm model with maximum adsorption capacity of 3,333.33 mg g^{-1} of Bi^{3+} on nano-HAp extracted from corals in acidic solution.

Acknowledgment This research was completely supported by Materials and Energy Research Center (MERC) under the project No. 371390051 for which the authors are grateful.

References

1. N. Tokman, S. Akman, Anal. Chim. Acta **519**, 87 (2004)
2. J.A. Reyes-Aguilera, M.P. Gonzalez, R. Navarro, T.I. Saucedo, M. Avila-Rodriguez, J. Membr. Sci. **310**, 13 (2008)
3. R. Pamphlett, M. Stoltenberg, J. Rungby, G. Danscher, Neurotoxicol. Teratol. **22**, 559 (2000)
4. I. Mobasherpour, E. Salahi, M. Pazouki, Desalination **266**, 142 (2011)
5. X.-B. Chen, J.V. Wright, J.L. Conca, L.M. Peurrung, Environ. Sci. Technol. **31**, 624 (1997)
6. V. Laperche, S.J. Traina, P. Gaddam, T.J. Logan, Environ. Sci. Technol. **30**, 3321 (1996)
7. Q.Y. Ma, S.J. Traina, T.J. Logan, J.A. Ryan, Environ. Sci. Technol. **27**, 1803 (1993)
8. Q.Y. Ma, S.J. Traina, T.J. Logan, J.A. Ryan, Environ. Sci. Technol. **28**, 1219 (1994)
9. E. Mavropoulos, A.M. Rossi, A.M. Costa, C.A.C. Perez, J.C. Moreira, M. Saldanha, Environ. Sci. Technol. **36**, 1625 (2002)
10. A. Nzihou, P. Sharrock, Waste Manag **22**, 235 (2002)
11. Y. Takeuchi, H. Arai, J. Chem. Eng. Jpn. **23**, 75 (1990)

12. J.A. Elliott, L. Tamarkin, J. Comp. Physiol. A **174**, 469 (1994)
13. H. Tanaka, M. Futaoka, R. Hino, K. Kandori, T. Ishikawa, J. Colloid Interface Sci. **283**, 609 (2005)
14. C.C. Fuller, J.R. Bargar, J.A. Davis, M.J. Piana, Environ. Sci. Technol. **36**, 158 (2001)
15. A.G. Leyva, J. Marrero, P. Smichowski, D. Cicerone, Environ. Sci. Technol. **35**, 3669 (2001)
16. S. McGrellis, J.-N. Serafini, J. JeanJean, J.-L. Pastol, M. Fedoroff, Sep. Purif. Technol. **24**, 129 (2001)
17. J. Reichert, J.G.P. Binner, J. Mater. Sci. **31**, 1231 (1996)
18. E.D. Vega, J.C. Pedregosa, G.E. Narda, J. Phys. Chem. Solids **60**, 759 (1999)
19. G. Guillemin, J.L. Patat, J. Fournie, M. Chetail, J. Biomed. Mater. Res. **21**, 557 (1987)
20. L. Merrill, W.A. Basset, Acta Crystallogr. **B31**, 343 (1975)
21. Z. Aksu, S. Tezer, Process Biochem. **40**, 1347 (2005)
22. W.J. Weber Jr, J.C. Morris, Am Soc Civil Eng **89**, 31 (1963)
23. I. Smičiklas, S. Dimović, I. Plećaš, M. Mitrić, Water Res. **40**, 2267 (2006)
24. S. Lu, S.W. Gibb, Bioresour. Technol. **99**, 1509 (2008)
25. Y.S. Ho, G. McKay, Process Biochem. **34**, 451 (1999)
26. M. Doğan, M. Alkan, Chemosphere **50**, 517 (2003)
27. Y.-S. Ho, Water Res. **37**, 2323 (2003)
28. Z. Aksu, Process Biochem. **38**, 89 (2002)
29. I. Langmuir, J. Am. Chem. Soc. **40**, 1361 (1918)
30. E. Malkoç, Y. Nuhoglu, Fresenius Environ. Bull. **12**, 376 (2003)
31. K. Kadirvelu, K. Thamaraiselvi, C. Namasivayam, Sep. Purif. Technol. **24**, 497 (2001)
32. S. Hasany, M. Saeed, M. Ahmed, J. Radioanal. Nucl. Chem. **252**, 477 (2002)
33. S. Khan, M. Williams, *Post-Tensioned Concrete Floors* (Butterworth-Heinemann, Oxford, 1995), p. 271
34. S.-H. Lin, R.-S. Juang, J. Hazard. Mater. **92**, 315 (2002)
35. C.-C. Wang, L.-C. Juang, C.-K. Lee, T.-C. Hsu, J.-F. Lee, H.-P. Chao, J. Colloid Interface Sci. **280**, 27 (2004)
36. B.S. Krishna, D.S.R. Murty, B.S. Jai Prakash, J. Colloid Interface Sci. **229**, 230 (2000)